

**Acknowledgements** We thank J. Dunn for technical assistance and J. Dunn, P. Zemrowski, A. Richter, C. Jarzab, H. Lang, R. Brown and A. Mergenthaler for field assistance. D.W. Schemske and S. J. Tonsor provided valuable comments on the manuscript. This work was supported by research grants from the National Science Foundation (USA) and the Research Development Fund of The University of Pittsburgh (S.K.).

**Competing interests statement** The authors declare that they have no competing financial interests.

**Correspondence** and requests for materials should be addressed to S.K. (kalisz@pitt.edu).

## A barley cultivation-associated polymorphism conveys resistance to powdery mildew

Pietro Piffanelli<sup>1\*†</sup>, Luke Ramsay<sup>2\*</sup>, Robbie Waugh<sup>2</sup>, Abdellah Benabdelmouna<sup>3</sup>, Angélique D'Hont<sup>3</sup>, Karin Hollricher<sup>4</sup>, Jørgen Helms Jørgensen<sup>5</sup>, Paul Schulze-Lefert<sup>6</sup> & Ralph Panstruga<sup>6</sup>

<sup>1</sup>The Sainsbury Laboratory, John Innes Centre, Colney Lane, Norwich NR4 7UH, UK

<sup>2</sup>Genomics Unit, Scottish Crop Research Institute, Invergowrie, Dundee DD2 5DA, UK

<sup>3</sup>CIRAD, Avenue Agropolis, 34398 Montpellier, Cedex 5, France

<sup>4</sup>Max-Planck-Institut für Züchtungsforschung, Department of Plant Breeding and Yield Physiology, Carl-von-Linne-Weg 10, D-50829 Köln, Germany

<sup>5</sup>Risø National Laboratory, Plant (formerly: Agricultural) Research Department, DK-4000 Roskilde, Denmark

<sup>6</sup>Max-Planck-Institut für Züchtungsforschung, Department of Plant–Microbe Interactions, Carl-von-Linne-Weg 10, D-50829 Köln, Germany

\* These authors contributed equally to this work

† Present address: CIRAD, Avenue Agropolis, 34398 Montpellier, Cedex 5, France

Barley (*Hordeum vulgare*) has played a pivotal role in Old World agriculture since its domestication about 10,000 yr ago<sup>1</sup>. Barley plants carrying loss-of-function alleles (*mlo*) of the *Mlo* locus are resistant against all known isolates of the widespread powdery mildew fungus<sup>2</sup>. The sole *mlo* resistance allele recovered so far from a natural habitat, *mlo-11*, was originally retrieved from Ethiopian landraces and nowadays controls mildew resistance in the majority of cultivated European spring barley elite varieties<sup>2</sup>. Here we use haplotype analysis to show that the *mlo-11* allele probably arose once after barley domestication. Resistance in *mlo-11* plants is linked to a complex tandem repeat array inserted upstream of the wild-type gene. The repeat units consist of a truncated *Mlo* gene comprising 3.5 kilobases (kb) of 5'-regulatory sequence plus 1.1 kb of coding sequence. These generate aberrant transcripts that impair the accumulation of both *Mlo* wild-type transcript and protein. We exploited the meiotic instability of *mlo-11* resistance and recovered susceptible revertants in which restoration of *Mlo* function was accompanied by excision of the repeat array. We infer *cis*-dependent perturbation of transcription machinery assembly by transcriptional interference in *mlo-11* plants as a likely mechanism leading to disease resistance.

Barley *Mlo* encodes the prototype of a plant-specific family of seven-transmembrane domain proteins<sup>3–5</sup>. The protein interacts with the Ca<sup>2+</sup> sensor calmodulin and seems to inhibit a vesicle-associated and SNARE-protein-dependent resistance to the barley powdery mildew fungus (*Blumeria graminis* f. sp. *hordei*; *Bgh*) at the cell periphery<sup>6–8</sup>. Each of 17 molecularly characterized *mlo* mutants was derived from chemical-induced or radiation-induced mutagenesis, invariably affecting coding or intron splice junction

sequences<sup>3,9</sup>. Some primitive cultivars (landraces) collected from the granaries of local farmers in Ethiopia during expeditions in 1937 and 1938 possess strong resistance against all tested *Bgh* isolates<sup>2,10</sup> that genetic analysis has attributed to the presence of *mlo* alleles (designated *mlo-11*; ref. 11). The frequency of this naturally occurring broad-spectrum resistance to powdery mildew was 0.2–0.6% in total Ethiopian landrace material but in a particular locality was up to a level of 24% (refs 2, 12).

In contrast to fully resistant mutagen-induced *mlo*-null mutants<sup>3</sup>, *mlo-11* plants allow the low-level growth of sporulating *Bgh* colonies (Fig. 1a). When homozygous *mlo-11* resistant plants were self-pollinated (selfing), fully susceptible individuals were recovered with a frequency of about  $(0.5–1) \times 10^{-4}$  (designated 'revertants'; Fig. 1a, Supplementary Table 1), indicating a possible meiotic instability of the *mlo-11* allele. In contrast, no susceptible individual was found in about 125,000 progeny obtained after selfings of *mlo* resistant lines containing various mutation-induced lesions in *Mlo* (Supplementary Table 1). Extensive genetic analysis of the susceptible *mlo-11* revertants indicated that either the *Mlo* susceptibility allele was restored or that susceptibility was the result of a heritable change in a tightly linked locus (Supplementary Table 2).

DNA sequencing of the *Mlo* coding region in *mlo-11* resistant plants failed to detect differences from the *Mlo* wild-type sequence. However, genomic Southern blots probed with full-size *Mlo* complementary DNA (cDNA) detected expected fragment sizes of wild-type *Mlo* and additional strongly hybridizing fragments (Fig. 1b). Similarly, six of seven Ethiopian broad-spectrum powdery-mildew-resistant accessions of the Centre for Genetic Resources of The Netherlands (Supplementary Table 3), included in the haplotype analysis described below, showed a genomic Southern pattern identical to *mlo-11* plants (not shown). The additional hybridizing signals were absent from both homozygous susceptible *mlo-11* revertant progeny and susceptible *Mlo* wild-type control plants (Fig. 1b), indicating a causal link between the presence of these additional *Mlo*-homologous fragments in *mlo-11* plants and resistance. Relative signal intensities suggested that the extra sequences were present in multiple copies. Polymerase chain reaction (PCR) analysis of *mlo-11* genomic DNA showed that these were arranged as tandem repeat units, consisting of 1.1 kb of *Mlo* coding sequence (exon 1 to intron 5) flanked by 3.5-kb upstream sequences (Fig. 2a, b). Juxtaposed repeats were separated by a GT dinucleotide (Fig. 2b) not present in wild-type *Mlo*. Quantitative real-time PCR analysis revealed  $9.4 \pm 4.2$  copies of the repeat unit in cultivar Ingrid BC *mlo-11*,  $1.0 \pm 0.3$  copies in the tested homozygous susceptible revertant line, and  $7.2 \pm 4.3$  copies in the tested homozygous resistant revertant sibling (all values relative to cultivar Ingrid *Mlo*, set as 1.0). The tandem repeat structure in *mlo-11* is reminiscent of concatemers generated by the 'rolling-circle' DNA replication used by some viruses and transposons present in plants, for example the geminiviruses<sup>13</sup> and *Helitron* transposons<sup>14</sup>. Chance use of a section of the *Mlo* gene by the rolling-circle DNA replication machinery offers a possible explanation for the presence of the *mlo-11* repeat array.

We constructed a genomic cosmid library from *mlo-11* plants and isolated four cosmid clones with the use of a *Mlo* 5'-terminal cDNA probe. DNA sequencing from the clones identified the 5' end of the repeat structure, consisting of a severely truncated repeat unit (Fig. 2d). Two low-copy loci located 5' of the repeat array were anchored to three of four *Mlo*-containing yeast artificial chromosome (YAC) clones, thereby unambiguously locating the *mlo-11* repeat structure upstream of and adjacent to wild-type *Mlo* (Fig. 2e). None of the cosmid clones contained the 3' end of the repeat structure, and PCR amplification of this region from genomic DNA failed. However, the 3' end is likely to be located at least 1.8 kb upstream of the wild-type *Mlo* copy because identically sized fragments (representing wild-type *Mlo*) were detected by Southern

blot analysis in wild-type and *mlo-11* mutant plants by using diverse restriction enzymes (Fig. 1b, 2c). In addition, contiguous fibre-FISH fluorescent signals in chromosome sets derived from *Mlo* and *mlo-11* lines provided direct experimental evidence for an immediate physical linkage of the *mlo-11* repeat array and the *Mlo* wild-type copy (Fig. 1c).

We rescued two independent *mlo-11* revertants from resistant *mlo-11* accessions that flowered at different times. Both revertants retained their respective flowering time phenotypes, supporting the notion of an independent origin of the revertants (Supplementary Fig. 1). Although Southern analysis seemingly indicated a complete loss of the *mlo-11* repeat units in both revertants (Fig. 1b), examination by PCR revealed the presence of the truncated version of the 5'-terminal *mlo-11* repeat unit, thereby providing a molecular

footprint of ancestry (Supplementary Fig. 1b, c). Loss of the repeat units in the susceptible revertants might be explained by unequal crossover events of the 5'-most repeat unit with the wild-type *Mlo* gene copy during meiosis, a mechanism that would be compatible with the observed meiotic reversion frequency and the detected terminal repeat remnant in both revertants.

Although the repeat array in *mlo-11* plants is reminiscent of repeat-induced gene silencing, a phenomenon associated with transgene tandem repeat copies in eukaryotes<sup>15</sup>, we failed to detect significant CpG methylation or evidence for altered chromatin configuration at the *Mlo* locus in *mlo-11* plants (Supplementary Fig. 2). Heterozygous *Mlo/mlo-11* plants (hemizygous for the *mlo-11* repeat array) are susceptible to *Bgh* (Supplementary Table 2). This finding and transient expression analysis (Supplementary Table 4)

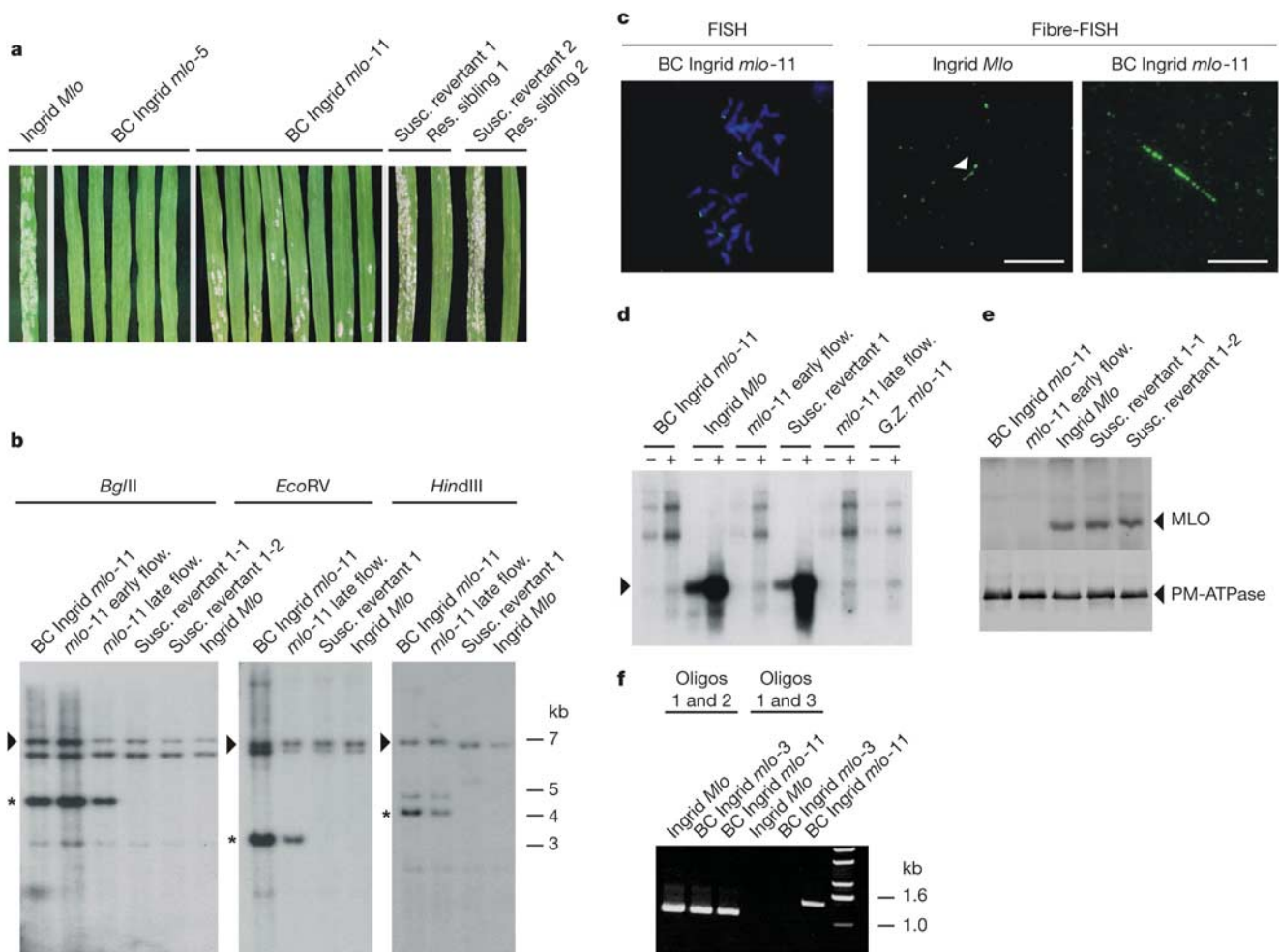


**Figure 1** Phenotypic and molecular characterization of barley *Mlo* wild-type plants, resistant *mlo-11* mutants, susceptible *mlo-11* revertants and their resistant siblings. **a**, *Bgh* infection phenotypes of barley seedlings. Susc. revertant, homozygous (*Mlo/Mlo*) susceptible offspring of the heterozygous (*Mlo/mlo*) susceptible revertant; res. sibling, homozygous (*mlo/mlo*) resistant offspring of the heterozygous (*Mlo/mlo*) susceptible revertant. **b**, Southern blot probed with a full-size *Mlo* cDNA fragment. Arrows indicate expected wild-type bands; asterisks indicate *mlo-11*-specific bands. Additional bands probably result from cross-hybridization with the sequence-related *HvMlo2* homologue (GenBank accession number Z95496). **c**, FISH and fibre-FISH analysis (see Methods). Arrowhead, hybridization signal in Ingrid *Mlo*; scale bars, 10  $\mu$ m (corresponds to about 30 kb). **d**, Northern blot of poly(A)<sup>+</sup> RNA from uninfected (–) or powdery-mildew-inoculated (+; samples taken 9 h after inoculation) barley seedlings probed with a full-size *Mlo* cDNA fragment. The arrowhead indicates the position of the ~2-kb *Mlo* wild-type

transcript. Note the aberrant high-molecular-mass transcripts in BC Ingrid *mlo-11*, *mlo-11* (late and early flowering) and G.Z. ('Grannenlose Zweizeilige') *mlo-11*. Susceptible revertant 1 is a homozygous (*Mlo/Mlo*) segregant of the susceptible heterozygous (*Mlo/mlo*) revertant obtained from *mlo-11* (late flowering) selfing. **e**, Western blot with protein extracts of enriched plasma membranes of uninfected barley seedlings probed with either MLO-specific (upper panel) or plasma membrane ATPase (PM-ATPase)-specific (lower panel) antisera as described previously<sup>4</sup>. **f**, RT-PCR analysis of RNA extracted from unchallenged barley seedlings with the use of the following oligonucleotides: 1, binds in *Mlo* cDNA downstream of repeat units, reverse primer; 2, binds in *Mlo* cDNA around the translational start site, forward primer; 3, binds at about –70 relative to the experimentally determined *Mlo* transcriptional start site<sup>3</sup>, forward primer.

reveals that the *mlo-11* repeat array does not interfere with the function of a wild-type *Mlo* copy *in trans*, thus excluding conventional post-transcriptional gene silencing as a potential interference mechanism. Inactivation of *Mlo* in *mlo-11* plants must therefore be fundamentally different from *trans*-acting epigenetic effects reported for the maize *b1* and *pericarp color1* loci, in which either tandem repeat units of 853 base pairs (bp) located 100 kb upstream of *b1* or the genetically unlinked *Unstable factor for orange1*, respectively, are required for epigenetic modification<sup>16,17</sup>.

Constitutive low-level transcription of the *Mlo* gene is known to be upregulated about tenfold on challenge with a pathogen<sup>9</sup>. Wild-type *Mlo* transcripts were undetectable in poly(A)<sup>+</sup> RNA isolated from unchallenged *mlo-11* resistant leaves (Fig. 1d). However, aberrant high-molecular-mass transcripts were observed that increased in abundance after challenge with a pathogen. At least part of these polyadenylated aberrant transcripts must originate from the supernumerary 5' regulatory sequences within the upstream *mlo-11* repeat units because we detected in reverse transcriptase PCR (RT-PCR) products of *mlo-11* RNA samples the *mlo-11*-specific GT dinucleotide that links adjacent repeat units at the DNA level (Fig. 1d, Supplementary Fig. 3). In addition, RT-PCR analysis provided direct evidence for transcriptional read-through of wild-type *Mlo* from upstream repeat units (Fig. 1f). Trace amounts of wild-type-sized transcripts were detectable in pathogen-challenged *mlo-11* leaves but these signals were still much weaker than those of wild-type transcripts in unchallenged susceptible *Mlo* plants (Fig. 1d). Transcript patterns in homozygous susceptible revertant progeny were undistinguishable from those in wild-type *Mlo* plants (Fig. 1d). Consistent with an essentially silent *Mlo* wild-type copy in *mlo-11* plants was our observation that western blot analysis failed to detect MLO protein in *mlo-11* mutants but revealed wild-type MLO concentrations in the homozygous susceptible revertants (Fig. 1e). These findings are strongly suggestive of a disruption of transcription machinery assembly by read-through into the wild-type *Mlo* copy from upstream repeat units in *mlo-11* plants<sup>18</sup>, a phenomenon not reported previously for a naturally occurring allele of a plant gene. The few powdery mildew colonies on *mlo-11* leaves (Fig. 1a) could indicate that the repeat-array-dependent transcriptional interference occasionally becomes 'leaky', an interpretation supported by the accumulation of very small amounts of wild-type-sized *Mlo* transcripts detected after challenge with a pathogen.

We performed haplotype analysis at the *Mlo* locus with a sample of 91 barley accessions comprising modern cultivated *H. vulgare*, undomesticated *H. spontaneum* ancestors, and cultivation intermediates represented by Ethiopian *H. vulgare* landraces. In a 25-kb interval including *Mlo* (ref. 19) we assayed eight sites exhibiting polymorphisms such as size variants of simple sequence repeats (SSRs) and the presence or absence of miniature transposable elements (MITEs). In addition, we monitored single-nucleotide polymorphisms (SNPs) as well as indels within the entire *Mlo* coding region (Supplementary Fig. 4 and Supplementary Table 5). In the cultivated accessions, three basic haplotypes (I–III) were observed that were distinct from one another across the entire interval (Fig. 3a). Representatives of each haplotype class were present both in early twentieth-century European varieties (I Binder, II Gull, III Hanna) and in more recently developed cultivars. A far greater number of haplotypes were identified within the *H. spontaneum* accessions (Fig. 3b). This pattern of diversity is consistent with a bottleneck associated with domestication when little of the genetic diversity of *H. spontaneum* was transferred to cultivated barley<sup>20</sup>. All *mlo-11* resistant Ethiopian landrace accessions and modern European cultivars that carry the introgressed *mlo-11* allele contained near-identical haplotypes that grouped with class I haplotypes of wild-type *Mlo* cultivars (Fig. 3a and Supplementary Table 5). This is strongly indicative of a monophyletic

origin of *mlo-11* and indicates that the allele probably emerged recently within a common barley haplotype after domestication. The absence of SNPs between different *mlo-11* repeat units is consistent with the inferred recent emergence of the mutant allele (not shown).

Null mutations in *Mlo* have undesirable pleiotropic effects including accelerated leaf senescence and reduced grain yield<sup>2,9</sup>, whereas the residual *Mlo* wild-type activity in *mlo-11* plants might reduce the severity of these effects. The southwestern part of Ethiopia, a region comprising highland areas with high rainfall, favours infections with powdery mildew<sup>12</sup>. The adverse effects associated with *mlo*-null mutations and the capacity of polymorphic race-specific resistance loci to contain *Bgh* epidemics (for example, natural variation at *Mla*; ref. 21) might have prevented the elimination of the *Mlo* wild-type allele in undomesticated *H. spontaneum*. The presence of the broad-spectrum *mlo-11* resistance allele in primitive Ethiopian landraces might be advantageous because it would compensate for the inherent erosion of natural

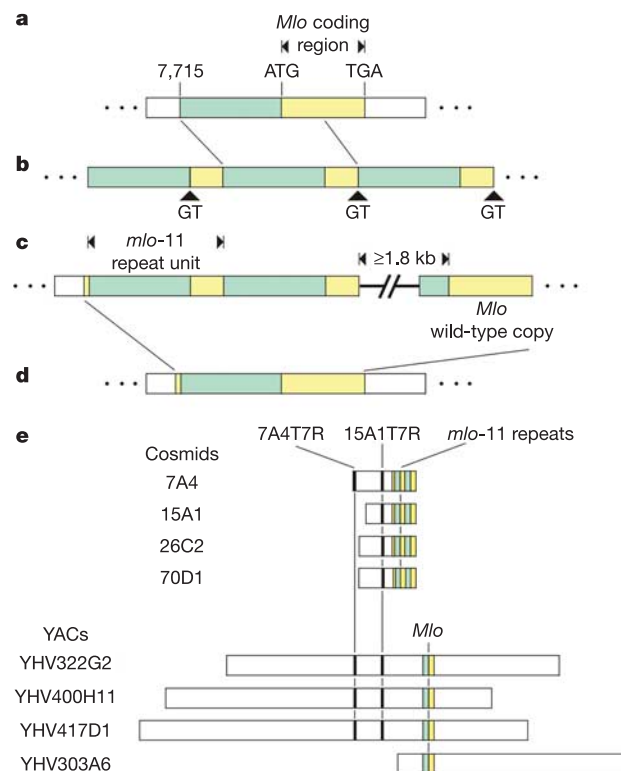


**Figure 2** Schematic representation of the *Mlo* locus and *mlo-11* repeat array organization. **a**, The rectangle symbolizes the genomic locus at *Mlo*. *Mlo* coding sequence (11,211–14,049, numbering according to GenBank accession no. Y14573) is marked by a yellow box, the *Mlo* upstream sequence that is part of the repeat units (7,715–11,210) is indicated by a blue box. Flanking genomic regions are depicted in white. **b**, Three (of about five to ten) consecutive *mlo-11* repeat units. Colour coding of boxes is as described above. For simplicity, *Mlo* intron sequences are not indicated. GT indicates the *mlo-11*-specific GT dinucleotide separating each repeat unit. **c**, Linkage of terminal repeat units with flanking genomic regions. The most upstream repeat unit is severely truncated and connects to the authentic *Mlo* locus upstream region. The connection between the most downstream repeat unit and the *Mlo* wild-type gene copy is not resolved. **d**, Organization of the *Mlo* locus in susceptible revertants. The truncated upstream repeat unit identifies the revertant as a genuine *mlo-11* descendant. **e**, Relative arrangement of cosmid clones 7A4, 15A1, 26C2 and 70D1, cosmid-derived markers 7A4T7R and 15A1T7R, and *Mlo*-containing YAC clones YHV322G2, YHV400H11, YHV417D1 and YHV303A6 (ref. 26). Clones are not drawn to scale.



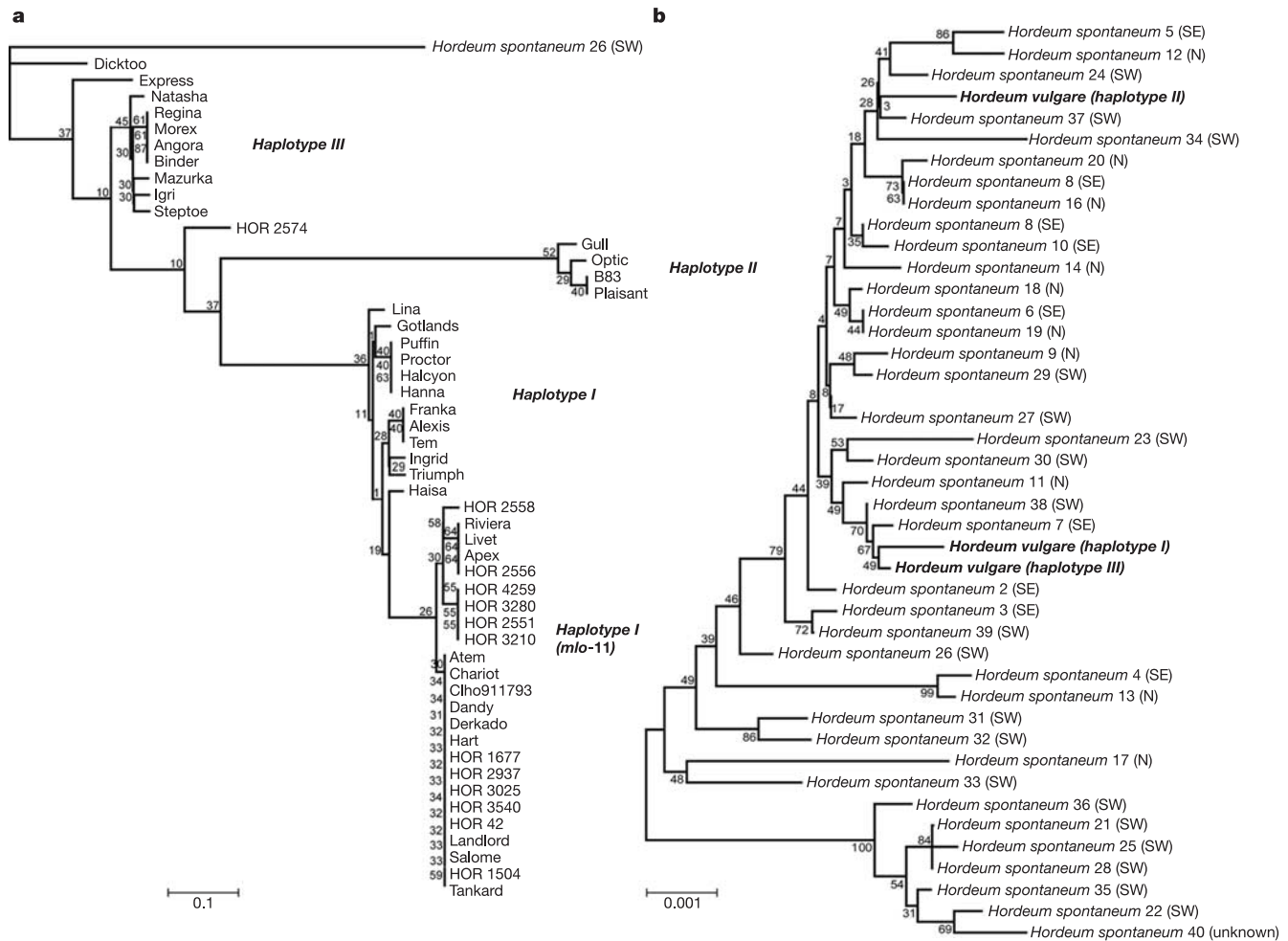


**Figure 3** Phylogenetic relationship of barley germplasm based on haplotype analysis at *Mlo*. **a**, Phylogenetic tree based on genotypes of SSR and MITE markers in a 25-kb interval around *Mlo*. The scale bar indicates Nei's standard genetic distance  $D_s$  (ref. 27). **b**, Phylogenetic tree based on SNPs and indels in the *Mlo* coding region

(including introns). The scale bar indicates nucleotide substitutions per position. On both trees, the numbers above nodes indicate bootstrap support based on 10,000 replicates.

genetic variation at race-specific resistance loci upon barley domestication. It remains to be tested whether the occurrence and distribution of beneficial *mlo-11* resistance in the Ethiopian highlands resulted from conscious or unconscious selection by local farmers, which in effect might have created a cultivation-associated balanced polymorphism (*Mlo/mlo-11*) in barley landraces. □

**Methods**

**Plant material**

The germplasm used for haplotype analysis included modern European cultivars, some winter but mostly spring types, a subset of which contain introgressed *mlo-11* (ref. 22), some Ethiopian landrace accessions (*mlo-11* types) including probable donors of the resistance to cultivars<sup>2</sup> and a range of *Hordeum vulgare spontaneum* lines from Israel, Turkey and Iran<sup>23</sup>. The Ethiopian landrace material was obtained from stock centres at the IPK Gatersleben (Germany), the Centre for Genetic Resources (Wageningen, The Netherlands) and the National Small Grains Collection (Aberdeen, Idaho, USA).

Barley genotypes Ingrid *Mlo*, backcross Ingrid (BC Ingrid) *mlo-11* and BC Ingrid *mlo-5* were kindly provided by J. MacKey (Uppsala, Sweden).

**Haplotype analysis and generation of phylogenetic trees**

In addition to a determination of the allelic variation at the *Mlo* locus by sequencing across all exons and introns (2,839 bp) the alleles were assayed at a range of putative polymorphic sites in the gene region. These included both SSRs and MITEs identified around the *Mlo* locus (Supplementary Fig. 4). SSR marker loci were amplified by PCR, respective products were resolved on polyacrylamide gels and the sizes of the products were estimated by reference to a SequaMark ladder (Research Genetics, Huntsville, Alabama, USA). The

MITE marker loci products were resolved on 1% agarose gels and the exact size differences were determined by sequencing of representative alleles. The polymorphisms found at these marker loci and within the gene sequence were combined to determine a haplotype of the *Mlo* region. The neighbour-joining tree shown in Fig. 3a was constructed with Populations version 1.2.28 (<http://www.cnrs-gif.fr/pge/bioinfo/populations/index.php>) using Nei's standard measure of distance  $D_s$ , and were visualized and drawn using Treeview version 1.6.6 (<http://taxonomy.zoology.gla.ac.uk/rod/treeview.html>). *H. spontaneum* 26 (SW) served as outgroup for generation of the tree. The neighbour-joining tree shown in Fig. 3b was constructed using MEGA2 software (<http://www.megasoftware.net>) with Kimura 2 parameter model, both transitions and transversions included and the pairwise deletion option. Detailed data used for the generation of both phylogenetic trees can be found in Supplementary Table 5.

**Generation of a *mlo-11* cosmid library**

Genomic DNA of barley line *mlo-11* (early flowering) was partly digested with restriction enzyme *Sau3AI* and ligated into linearized (*Bam*HI) and dephosphorylated cosmid vector SuperCos1 (Stratagene, La Jolla, California, USA). Recombinant clones were found to carry inserts of about 30–42 kb and were sampled in 220 pools, each consisting of about 4,000 clones. Thus, the cosmid library represents about five barley genome equivalents (30 kb per clone × 220 pools × 4,000 clones ≈ 26.4 megabases (Mb); the barley genome size is about 5.3 Mb). The DNA sequence of presumptive (according to BLAST analysis) single/low-copy end fragments of cosmids 7A4 and 15A1 was exploited to derive oligonucleotides suitable for PCR amplification of the respective loci from genomic DNA.

**Quantitative real-time PCR**

Quantitative real-time PCR was used to estimate the number of *mlo-11* repeat units in genomic DNA of various barley genotypes. Oligonucleotide combinations that either specifically amplify *mlo-11* repeat DNA or a single-copy *Mlo* carboxy-terminal fragment

(serving as an internal standard) were used in independent reactions performed on an ABI PRISM 7700 Sequence Detection System (Applied Biosystems, Foster City, California, USA). Data were analysed by the comparative  $\Delta\Delta C_T$  method (ABI PRISM 7700 User Bulletin) and represent means and standard deviations of five independent amplifications with two to four replicates each.

**FISH and fibre-FISH analysis**

Two mitotic metaphase chromosome sets of root tips derived from germinated seedlings of line BC Ingrid *mlo-11* were hybridized *in situ*<sup>24</sup> with a 4.5-kb *mlo-11* repeat unit fragment to demonstrate the specificity of this probe. For fibre-FISH analysis, nuclei were isolated from barley young leaves, fibres were prepared and stretched with the tilting method<sup>25</sup> and were subsequently hybridized with the 4.5-kb *mlo-11* repeat unit fragment.

Received 3 May; accepted 23 June 2004; doi:10.1038/nature02781.

1. Badr, A. *et al.* On the origin and domestication history of barley (*Hordeum vulgare*). *Mol. Biol. Evol.* **17**, 499–510 (2000).
2. Jørgensen, J. H. Discovery, characterization and exploitation of *Mlo* powdery mildew resistance in barley. *Euphytica* **63**, 141–152 (1992).
3. Büschges, R. *et al.* The barley *Mlo* gene: A novel control element of plant pathogen resistance. *Cell* **88**, 695–705 (1997).
4. Devoto, A. *et al.* Topology, subcellular localization, and sequence diversity of the *Mlo* family in plants. *J. Biol. Chem.* **274**, 34993–35004 (1999).
5. Devoto, A. *et al.* Molecular phylogeny and evolution of the plant-specific seven-transmembrane MLO family. *J. Mol. Evol.* **56**, 77–88 (2003).
6. Panstruga, R. & Schulze-Lefert, P. Corruption of host seven-transmembrane proteins by pathogenic microbes: a common theme in animals and plants? *Microbes Infect.* **5**, 429–437 (2003).
7. Kim, M. C. *et al.* Calmodulin interacts with MLO protein to regulate defence against mildew in barley. *Nature* **416**, 447–450 (2002).
8. Collins, N. C. *et al.* SNARE-protein-mediated disease resistance at the plant cell wall. *Nature* **425**, 973–977 (2003).
9. Piffanelli, P. *et al.* The barley MLO modulator of defense and cell death is responsive to biotic and abiotic stress stimuli. *Plant Physiol.* **129**, 1076–1085 (2002).
10. Giessen, J. E., Hoffmann, W. & Schottenloher, R. Die Gersten Äthiopiens und Erythraäs. *Z. Pflanzenzüchtung* **35**, 377–440 (1956).
11. Jørgensen, J. H. in *Barley Genetics III* (ed. Gaul, H.) 446–455 (Karl Thieme, München, 1976).
12. Negassa, M. Geographic distribution and genotypic diversity of resistance to powdery mildew of barley in Ethiopia. *Hereditas* **102**, 113–121 (1985).
13. Gutierrez, C. Geminivirus DNA replication. *Cell. Mol. Life Sci.* **56**, 313–329 (1999).
14. Kapitonov, V. V. & Jurka, J. Rolling-circle transposons in eukaryotes. *Proc. Natl Acad. Sci. USA* **98**, 8714–8719 (2001).
15. Henikoff, S. Conspiracy of silence among repeated transgenes. *BioEssays* **20**, 532–535 (1998).
16. Stam, M., Beale, C., Dorweiler, J. E. & Chandler, V. L. Differential chromatin structure within a tandem array 100 kb upstream of the maize *b1* locus is associated with paramutation. *Genes Dev.* **16**, 1906–1918 (2002).
17. Chopra, S. *et al.* The maize *Unstable factor for orange1* is a dominant epigenetic modifier of a tissue specifically silent allele of *pericarp color1*. *Genetics* **163**, 1135–1146 (2003).
18. Eszterhas, S. K., Bouhassira, E. E., Martin, D. I. K. & Fiering, S. Transcriptional interference by independently regulated genes occurs in any relative arrangement of the genes and is influenced by chromosomal integration position. *Mol. Cell. Biol.* **22**, 469–479 (2002).
19. Panstruga, R., Büschges, R., Piffanelli, P. & Schulze-Lefert, P. A contiguous 60 kb genomic stretch from barley reveals molecular evidence for gene islands in a monocot genome. *Nucleic Acids Res.* **26**, 1056–1062 (1998).
20. Matus, I. A. & Hayes, P. M. Genetic diversity in three groups of barley germplasm assessed by simple sequence repeats. *Genome* **45**, 1095–1106 (2002).
21. Jørgensen, J. H. Genetics of powdery mildew resistance in barley. *Crit. Rev. Plant Sci.* **13**, 97–119 (1994).
22. Pakniyat, H. *et al.* AFLP variation in wild barley (*Hordeum spontaneum* C. Koch) with reference to salt tolerance and associated ecogeography. *Genome* **40**, 332–341 (1997).
23. Thomas, W. T. B. *et al.* Identification of a QTL decreasing yield in barley linked to *Mlo* powdery mildew resistance. *Mol. Breed.* **4**, 381–393 (1998).
24. Benabdelmoua, A., Abirached-Darmency, M. & Darmency, H. Phylogenetic and genomic relationships in *Setaria italica* and its close relatives based on the molecular diversity and chromosomal organization of 5S and 18S–5.8S–25S rDNA genes. *Theor. Appl. Genet.* **103**, 668–677 (2001).
25. Frasz, P. F. *et al.* High-resolution physical mapping in *Arabidopsis thaliana* and tomato by fluorescence *in situ* hybridization to extended DNA fibers. *Plant J.* **9**, 421–430 (1996).
26. Simons, G. *et al.* AFLP-based fine mapping of the *Mlo* gene to a 30-kb DNA segment of the barley genome. *Genomics* **44**, 61–70 (1997).
27. Nei, M. Genetic distance between populations. *Am. Nat.* **106**, 283–292 (1972).

**Supplementary Information** accompanies the paper on [www.nature.com/nature](http://www.nature.com/nature).

**Acknowledgements** We thank B. Koop, C. Casais, I. Tierney and M. Macaulay for technical assistance; I. Somssich for experimental proposals; and N. Collins and M. Koornneef for suggestions on the manuscript. This work was supported by grants from the Gatsby Charitable Foundation to P.S.-L., from the Max-Planck Society to R.P., from Génoplatte to A.B., and from the Scottish Executive Environment and Rural Affairs Department and the European Commission to R.W.

**Competing interests statement** The authors declare that they have no competing financial interests.

**Correspondence** and requests for materials should be addressed to P.S.-L. (schlef@mpiz-koeln.mpg.de).

.....  
**SNF-6 is an acetylcholine transporter interacting with the dystrophin complex in *Caenorhabditis elegans***

Hongkyun Kim<sup>1</sup>, Matthew J. Rogers<sup>1</sup>, Janet E. Richmond<sup>2</sup> & Steven L. McIntire<sup>1</sup>

<sup>1</sup>Ernest Gallo Clinic and Research Center, Programs in Neuroscience and Biomedical Sciences, Department of Neurology, University of California at San Francisco, 5858 Horton Street, Suite 200, Emeryville, California 94608, USA  
<sup>2</sup>Department of Biological Sciences, University of Illinois at Chicago, Chicago, Illinois 60607, USA

Muscular dystrophies are among the most common human genetic diseases and are characterized by progressive muscle degeneration. Muscular dystrophies result from genetic defects in components of the dystrophin–glycoprotein complex (DGC), a multimeric complex found in the muscle cell plasma membrane<sup>1</sup>. The DGC links the intracellular cytoskeleton to the extracellular matrix and is thought to be important for maintaining the mechanical integrity of muscles<sup>2</sup> and organizing signalling molecules<sup>3</sup>. The exact role of the DGC in the pathogenesis of disease has, however, remained uncertain<sup>4</sup>. Mutations in *Caenorhabditis elegans* DGC genes lead to specific defects in coordinated movement and can also cause muscle degeneration<sup>5–7</sup>. Here we show that mutations in the gene *snf-6* result in phenotypes indistinguishable from those of the DGC mutants, and that *snf-6* encodes a novel acetylcholine/choline transporter. SNF-6 mediates the uptake of acetylcholine at neuromuscular junctions during periods of increased synaptic activity. SNF-6 also interacts with the DGC, and mutations in DGC genes cause a loss of SNF-6 at neuromuscular junctions. Improper clearing of acetylcholine and prolonged excitation of muscles might contribute to the pathogenesis of muscular dystrophies.

In a genetic screen<sup>8</sup>, we identified 12 mutants exhibiting a locomotory phenotype (defect in coordinated movement) indistinguishable from that of *dys-1* (a dystrophin homologue) mutants. These mutants consist of two alleles of *dys-1*, two alleles of *dyb-1* (a dystrobrevin homologue), three alleles of *dyc-1* (a dystrophin and CAPON-related gene) and five alleles of a previously uncharacterized gene (*eg28*, *eg114*, *eg115*, *eg121* and *eg137*). All of these mutants exhibit a locomotory phenotype distinct from that of other locomotion-defective mutants. During slow basal movements these mutants show essentially wild-type locomotory behaviours; however, when the mutants are forced to move forwards rapidly in response to mechanical stimulation, they exhibit exaggerated bending of the anterior body and head, and mild hypercontraction (Fig. 1; Supplementary videos 1, 2, 3, 5 and 6). Hypercontraction of body muscles is known to result from increased synaptic concentrations of acetylcholine at the neuromuscular junction (NMJ) in *C. elegans*. In fact, *dys-1* and *dyb-1* mutants are known to be mildly hypersensitive to aldicarb, an inhibitor of acetylcholinesterases that enhances muscle contraction, indicating elevated cholinergic synaptic transmission<sup>5,6</sup>. *eg28* animals are also hypersensitive to aldicarb in comparison with wild-type animals (percentage paralysis of wild-type and *eg28* animals to 1 mM aldicarb:  $3.3 \pm 2.9$  and  $11.7 \pm 2.9$  at 50 min;  $20 \pm 5$  and  $35 \pm 0$  at 60 min;  $38.3 \pm 2.8$  and  $55 \pm 8.7$  at 70 min,  $P < 0.02$ ). Furthermore, we were able to phenocopy the locomotory defect of these mutants by short-term exposure of wild-type animals to aldicarb (Fig. 1a). Together these observations indicate that the locomotory defect of these mutants might be due to elevated concentrations of acetylcholine at the NMJ.

To gain insight into the underlying abnormality of this class of